

---

## FULLERENES AND ATOMIC CLUSTERS

---

# Dimension of Mesogenic Molecules as Atomic Clusters

E. M. Aver'yanov

Kirensky Institute of Physics, Siberian Division, Russian Academy of Sciences,  
Akademgorodok, Krasnoyarsk, 660036 Russia

e-mail: aver@iph.krasn.ru

Received February 24, 2004

**Abstract**—The problem regarding the mass dimension  $D$  of mesogenic molecules as atomic clusters is formulated and solved using computer simulation and analytical calculations. For a large number of compounds belonging to different chemical classes, it is shown that the cores of discotic lacunar (rodlike, lathlike) molecules forming nematic or columnar discotic (calamitic) phases have a fractional dimension  $1 < D_c < 2$  ( $D_c \approx 1$ ). The dependences of the dimension  $D_c$  on the symmetry, the conformation, and the structural–chemical features of the molecular core are determined. It is demonstrated that, in the region of side flexible chains in molecules of both types, the dimension  $D_{ch}$  can be either smaller or larger than unity, depending on the chain conformation. An analytical expression accounting for the results of numerical experiments is obtained for the dimension  $D_{ch}$ . © 2005 Pleiades Publishing, Inc.

### 1. INTRODUCTION

In recent years, considerable attention has been focused on the physical and chemical properties of nanoparticles and their clusters with a fractional mass dimension  $D < 3$  [1, 2]. In this respect, investigation into the dimension of the molecules treated as atomic clusters is an important problem. This problem is of special interest for mesogenic molecules that consist of tens or hundreds of atoms and are characterized by a wide variety of chemical structures and shapes [3–9]. These factors are primarily responsible for the character of molecular packing in the condensed state, the anisotropy of the local coordination environment of molecules, and the type of liquid crystals (calamitic, discotic) and their mesophases (nematic, smectic, columnar).

The shape of the molecules reflects the distribution of force centers throughout the molecular volume and affects the anisotropy of intermolecular interactions, the intermolecular correlations, the degree of orientational ordering of the molecules in a liquid crystal, the interrelation between the orientational and conformational degrees of freedom of the molecules, and the character of phase transitions. For example, discotic molecules, as a rule, have a planar central aromatic core with radial, relatively long, flexible aliphatic chains [5, 10]. The loose (lacunar [1]) structure of discotic molecules with the statistical symmetry axis  $C_k$  ( $k \geq 2$ ) is characterized by large-sized lacunas (holes, cavities) between the core fragments or side chains and a large free volume per chain. It should be noted that the free volume increases with an increase in the chain length. This structure enhances the high conformational mobility of the chains. In turn, the high conformational mobility manifests itself both in the temperature depen-

dence of the orientational order parameter of molecules  $S(T)$  for discotic nematic liquid crystals  $N_D$  [11, 12] and in a decrease in the orientational order parameter  $S$  in the phases  $N_D$  and  $N_{Dre}$  with an increase in the chain length [13, 14].

The difference between the mass dimensions  $D$  of discotic lacunar molecules in the regions of the molecular core and side chains can account for the large differences between the orientational order parameters  $S$ , which are observed experimentally [11–14] and predicted by modern variants of the molecular-statistical theory and computer simulation for discotic nematic liquid crystals  $N_D$  (see [14] and references therein). In a recent paper [14], I analyzed these data, formulated a problem regarding the dimension of real discotic molecules, and made the assumption that the mass dimension  $D$  of these molecules is less than 2.

The purpose of this paper is to investigate both numerically and analytically the mass dimension for a representative set of known lathlike and lacunar mesogenic molecules of different chemical classes and to elucidate how the dimension of these molecules  $D_c$  (in the core region) and  $D_{ch}$  (in the region of side chains) depends on the symmetry, the size, the structural–chemical features, the conformation of molecular core fragments, and the length and conformation of the chains. The specific features of the objects under investigation and the technique of their computer simulation are considered in Section 2. The results of numerical treatment of the dimension  $D_c$  are presented and analyzed in Section 3. The results of numerical and analytical investigations of the dimension  $D_{ch}$  are discussed in Section 4. The main results obtained in this work and the conclusions drawn are briefly summarized in Section 5.

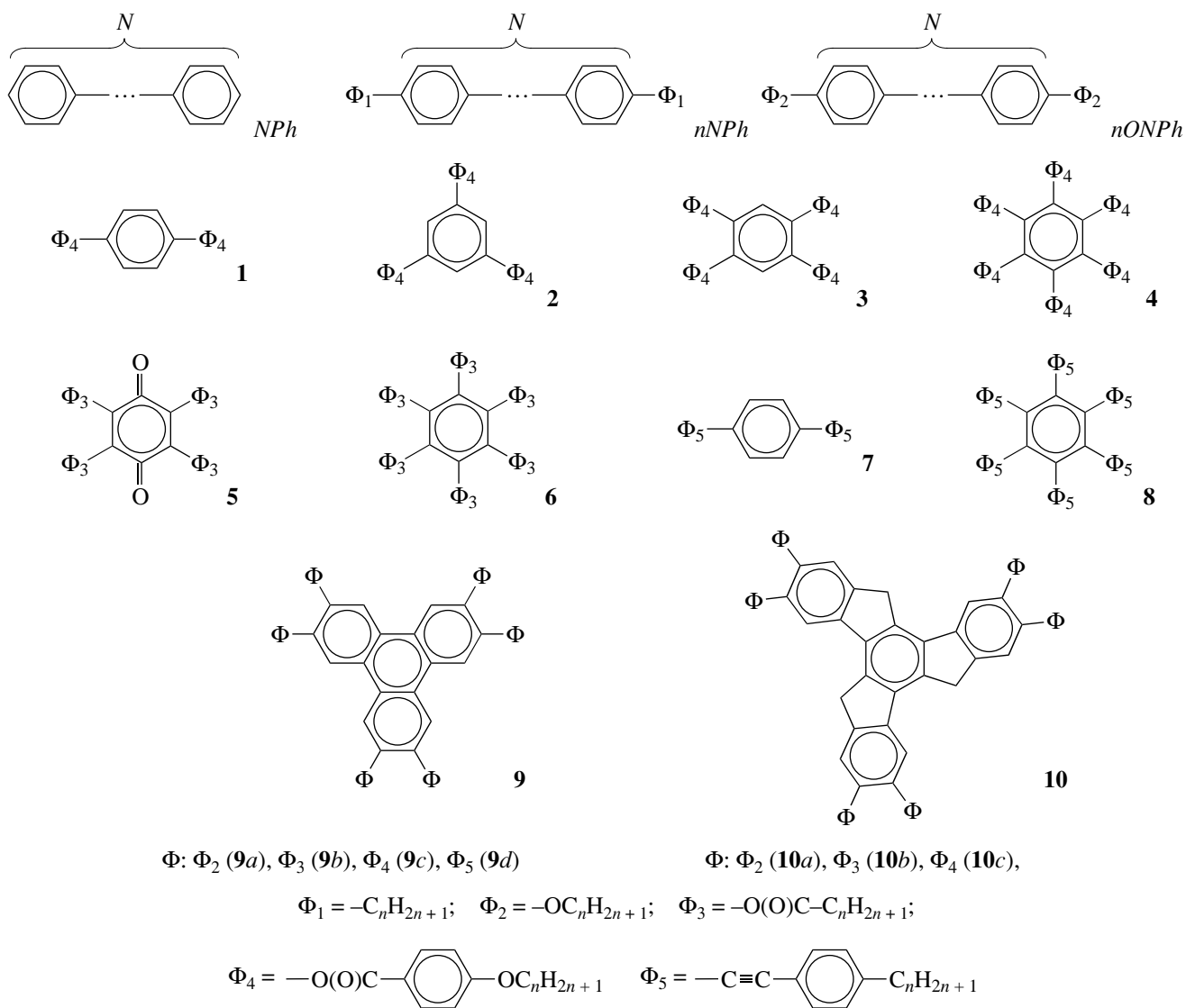


Fig. 1. Objects of investigation.

## 2. OBJECTS OF INVESTIGATION AND THEIR MODELS

The structural formulas of the studied compounds are presented in Fig. 1. These are the symmetrical molecules *NPh* [4, 7], *nNPh* [4, 15], and *nONPh*; molecules **1** and **7** [15] with rodlike or lathlike cores, which are abundant among calamitic liquid crystals; discotic molecules **2** [3, 16] and **3** [3, 4, 6]; model molecule **4** (for comparison with molecules **1–3**); and well-known molecules **5**, **6**, **8**, **9a–9d**, and **10a–10c** [3–7, 10], which form nematic and (or) columnar liquid-crystal phases. The orientational ordering of the usual, reentrant, or inverse nematic liquid-crystal phases was investigated for a number of homologs of compounds **8** [11, 12], **9c** [14], and **10b** [12, 13]. The chosen set include compounds with discotic molecules that have twofold (**3**, **5**), threefold (**2**, **9**, **10**), and sixfold (**4**, **6**, **8**) statistical

symmetry axes  $C_k$ . It should be noted that, in each of the three core fragments related by the symmetry axis  $C_3$  in molecules **10a–10c**, two  $\Phi$  fragments occupy symmetrically nonequivalent positions. The discotic molecules under consideration differ both in the structure, size, and lacunarity of the central core fragment and in the structure of the  $\Phi_1$ – $\Phi_5$  fragments whose attachment differently increases the transverse size of the core and the degree of its lacunarity.

In order to avoid details that are immaterial for the qualitative and quantitative results of the analysis, each molecule is simulated by a cluster consisting of identical spherical atoms of radius  $r$  whose centers coincide with the centers of carbon and oxygen atoms in the core and alkyl (alkyloxy) chains of the molecule without regard for the differences between the van der Waals radii of the carbon and oxygen atoms and the CH, CH<sub>2</sub>,

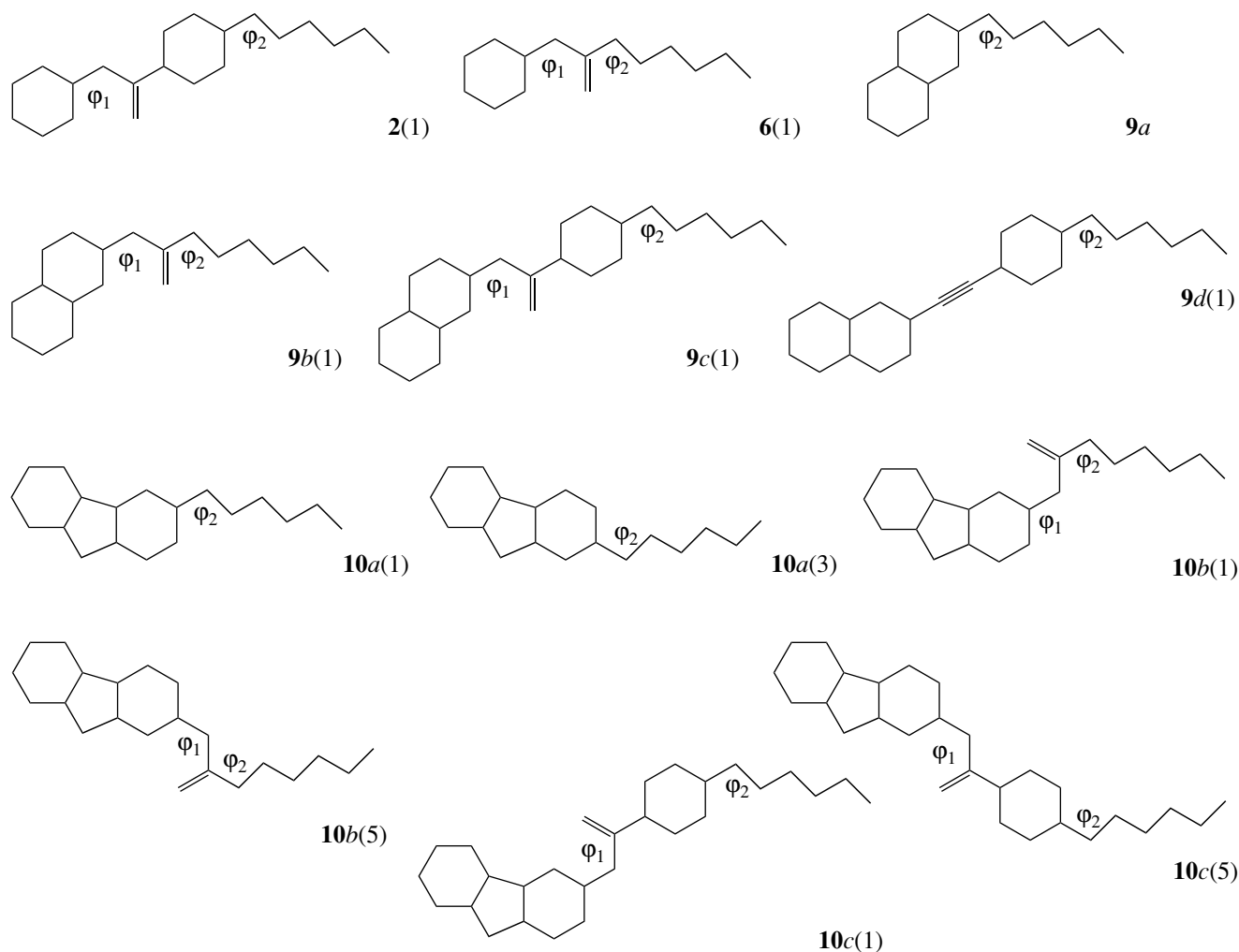


Fig. 2. Conformers of the side molecular fragments in the studied compounds.

and  $\text{CH}_3$  groups. The lengths of all the bonds C–C, C=C, C–O, and C=O are assumed to be  $l = 2r$ . All bond angles in the molecular cores and in the  $\Phi_k$  fragments are taken to be equal to  $120^\circ$  (except for molecules **10a–10c** with regular pentagons and hexagons in the core), and the C–C–C bond angles in the alkyl chains are assumed to be equal to a tetrahedral angle of  $109.47^\circ$ . Hereafter, all the linear sizes will be given in conventional units that correspond to  $r = 3.5$ .

The main conformations of the  $\Phi_k$  fragments with six (five) carbon atoms in the alkyl (alkyloxy) chains are shown in Fig. 2. The other conformations obtained from the main conformations by varying either the angle  $\varphi_1$  between the planes of the C(O)O group and the O-phenyl ring of the core or the angle  $\varphi_2$  between the plane of the carbon backbone of the side alkyl (alkyloxy) chain in the *trans* conformation and the plane of the phenyl ring or the C(O)O group bonded to this chain are listed in Table 1. For all the conformers containing the  $\Phi_4$  fragment, the plane of the C(O)O group

coincides with the plane of the C-phenyl ring bound to this group. In what follows, we will use designations of the type **9b(1/3)**. This designation means that, in each of the three core fragments in molecule **9b**, one  $\Phi_3$  fragment has conformation **9b(1)** and another  $\Phi_3$  fragment has conformation **9b(3)**; in this case, identical conformers in each core fragment are related by the molecular symmetry axis  $C_3$ . It should be noted that the results given below do not depend on the angle  $\varphi_1(\varphi_2)$  for molecules **1–6** [*nNPh*, *nOPh*, **7**, **8**, conformers **9b(1)**, **9b(2)**, **9c(1)**, **9c(2)**] or on the dihedral angles between the phenyl rings for molecules *NPh*, *nNPh*, and *nOPh*.

The number  $N(R)$  of spherical atoms inside the sphere of radius  $R$  whose center coincides with the center of the molecular core is counted in the numerical experiment. Since the atoms have identical mass, the mass  $M(R)$  of the part of the molecule within the sphere varies as  $M(R) \sim N(R)$ . For the  $\Phi_3$  ( $\Phi_4$ ,  $\Phi_5$ ) fragments, it is assumed that the C(O)O group (phenyl ring) enters into the composition of the molecular core. The core

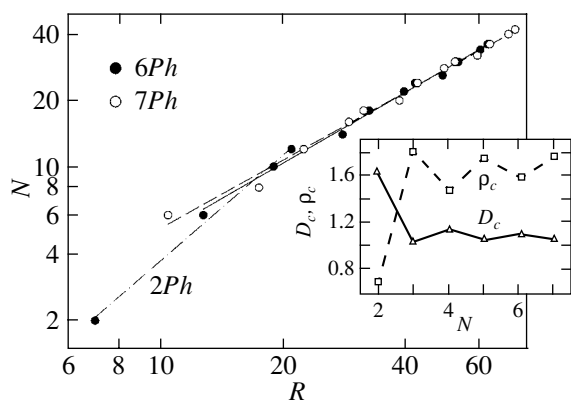


**Fig. 3.** Dependence  $N(R)$  for  $NPh$  molecules. The inset shows the dependences of the parameters  $\rho_c$  and  $D_c$  on the number  $N$  of phenyl rings in the same molecules.

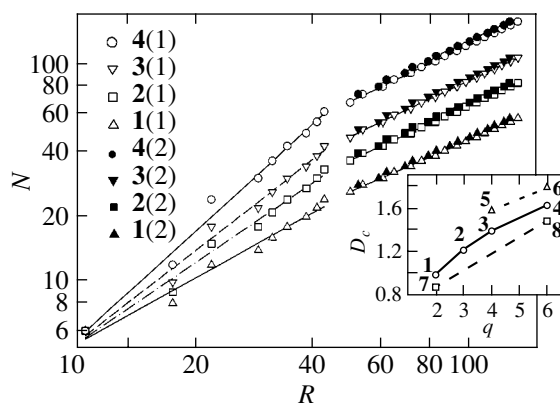


**Fig. 4.** Dependences  $N(R)$  for compounds **1–8**. The inset shows the dependences of the parameter  $D_c$  on the number  $q$  of radial core fragments for molecules **1–8**.

radii  $R_c$  and the numbers of atoms in the cores  $N_c = N(R_c)$  for the conformers of the compounds under consideration are presented in Table 2.

### 3. DIMENSION OF MOLECULES IN THE CORE REGION

The dependences of  $\log N(R)$  on  $\log R$  are characterized by the derivative

$$D(R) = \frac{d \ln N(R)}{d \ln R}. \quad (1)$$

For all the compounds and their conformers under investigation, the dependences of  $\log N(R)$  on  $\log R$

exhibit two linear portions with different derivatives  $D(R) \approx \text{const}$  in the core region ( $R \leq R_c$ ) and the region of side chains ( $R > R_c$ ). In the core region, these dependences in all the cases are described well by the relationship

$$\log N(R) = a_c + D_c \log R \quad (2)$$

with constant coefficients  $a_c$  and  $D_c$ . The observed deviations of a number of points from this dependence are primarily caused by the inclusion of the values of  $R$  for which the quantity  $N(R)$  changes by an integral number of atoms. The use of a continuous function  $M(R)$  leads to a smoothing of these deviations. In the range  $R \leq R_c$ ,

**Table 1.** Dihedral angles of the conformers under investigation

Conformer	<b>2(1)</b>	<b>2(2)</b>	<b>6(1)</b>	<b>6(2)</b>	<b>9a</b>	<b>9b(1)</b>	<b>9b(2)</b>	
$\varphi_1$	0–2 $\pi$		0–2 $\pi$		–	0		
$\varphi_2$	0	$\pm\pi$	0	$\pm\pi$	0	0	$\pm\pi$	
Conformer	<b>9b(3)</b>	<b>9b(4)</b>	<b>9c(1)</b>	<b>9c(2)</b>	<b>9c(3)</b>	<b>9c(4)</b>	<b>9d(1)</b>	
$\varphi_1$	$\pm\pi$		0		$\pm\pi$		–	
$\varphi_2$	0	$\pm\pi$	0	$\pm\pi$	0	$\pm\pi$	0	
Conformer	<b>9d(2)</b>	<b>10a(1)</b>	<b>10a(2)</b>	<b>10a(3)</b>	<b>10a(4)</b>	<b>10b(1)</b>	<b>10b(2)</b>	
$\varphi_1$	–	–					0	
$\varphi_2$	$\pm\pi$	0	$\pm\pi$	0	$\pm\pi$	0	$\pm\pi$	
Conformer	<b>10b(3)</b>	<b>10b(4)</b>	<b>10b(5)</b>	<b>10b(6)</b>	<b>10b(7)</b>	<b>10b(8)</b>	<b>10c(1)</b>	
$\varphi_1$	$\pm\pi$		0		$\pm\pi$		0	
$\varphi_2$	$\pm\pi$	0	0	$\pm\pi$	$\pm\pi$	0	0	
Conformer	<b>10c(2)</b>	<b>10c(3)</b>	<b>10c(4)</b>	<b>10c(5)</b>	<b>10c(6)</b>	<b>10c(7)</b>	<b>10c(8)</b>	
$\varphi_1$	0	$\pm\pi$		0		$\pm\pi$		
$\varphi_2$	$\pm\pi$	$\pm\pi$	0	0	$\pm\pi$	$\pm\pi$	0	

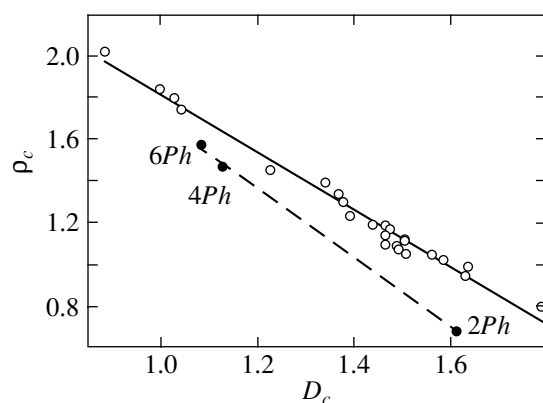


Fig. 5. Correlation between the parameters  $\rho_c$  and  $D_c$  in expression (3) for the studied compounds.

the dependence  $N(R)$  can be approximated by the expression

$$N(R) = \rho_c (R/r)^{D_c} \quad (3)$$

with the fractional dimension  $D = D_c$ . The prefactor  $\rho_c$  characterizes the density of infill of the molecular core with atoms and depends on the shape and chemical structure of the core. The coefficients of relationship (2) were determined using the option of the Statistics (Linear Regression) of the Sigma Plot 8.0 software package. The parameters  $\rho_c$  and  $D_c$  for the compounds under investigation are given in Table 2. The parameters  $D_c$  for molecules  $NPh$ ,  $nNPh$ , and  $nONPh$  with  $N \geq 3$  are obtained by ignoring the data at  $R = 7$  and  $N = 2$ .

It can be seen from Fig. 3 and the data presented in Table 2 that the values of  $D_c$  for molecules  $NPh$ ,  $nNPh$ ,  $nONPh$  ( $N \geq 3$ ), and **1** are close to unity. This is consistent with the linear shape of these molecules. A decrease in the width of molecule **7** (the appearance of lacunas) between the central and terminal phenyl rings of the core results in a decrease in the parameter  $D_c$  to 0.885, whereas the presence of two adjacent planar phenyl rings in the cores of molecules  $2Ph$ ,  $n2Ph$ , and  $nO2Ph$  leads to a considerable increase in the parameter  $D_c$ . As a result, the cores of these molecules become similar to the cores of discotic molecules. The even-odd alternation of the parameters  $\rho_c(N)$  and  $D_c(N)$  for molecules  $NPh$  with a variation in the number  $N$  of phenyl rings (see inset to Fig. 3) indicates a difference between the properties of the first compounds with even and odd values of  $N$  in this series and also a high sensitivity of the parameters  $\rho_c$  and  $D_c$  to similar structural features of the core.

Judging from the parameters  $1 < D_c < 2$  obtained for the discotic compounds, the disklike shape acceptable in the literature for their molecules does not correspond to the actual shape, because the disklike (disk-shaped) molecules should be described by expression (3) at  $D_c = 2$ . It seems likely that the loose structure of dis-

cotic molecules can be more precisely defined as a lacunar structure.

Let us consider the dependence of the parameter  $D_c$  on the number  $q$  of radial core fragments and the parameters  $R_c$  and  $N_c$ . At  $R_c = \text{const}$ , an increase in the parameter  $N_c$  and the number  $q$  of  $\Phi_4$  fragments in the series of compounds **1–2–3–4** leads to an almost linear increase in the parameter  $D_c(q)$  and an irregular change in the index  $k$  of the symmetry axis  $C_k$  of the molecule. A similar increase in the parameter  $D_c$  is observed with an increase in the number of  $\Phi_5$  ( $\Phi_3$ ) fragments from two (four) to six upon transition **7**  $\rightarrow$  **8** (**5**  $\rightarrow$  **6**). Note that the slopes of the curves  $D_c(q)$  in the above three cases are close to each other (see inset to Fig. 4). Owing to the denser infill of the circle of radius  $R$  with core fragments due to an increase in their number  $q$ , the parameter  $D_c$  tends to 2.

For  $q = \text{const}$ , an increase in the parameter  $R_c$  in the series **6–4–8** (**5–3**) is accompanied by an increase in the size of lacunas between the core fragments and a decrease in the parameter  $D_c$ . A similar situation is observed in the series **9b(1, 2)–9c(1, 2)–9d(1, 2)**. An increase in the lacuna size and the corresponding decrease in the parameter  $D_c$  also occur upon transition **9a**  $\rightarrow$  **10a** (**9b**  $\rightarrow$  **10b**, **9c**  $\rightarrow$  **10c**) for molecules containing identical substituting fragments  $\Phi$  due to the larger parameters  $R_c$  and the greater looseness of the unsubstituted core of molecule **10** as compared to the core of unsubstituted molecule **9**. However, the transition from conformer **10b** to conformer **10c** or **9c** leads to an increase in the parameter  $D_c$ , because the relative increase in  $N_c$  is larger than that in  $R_c$ .

For  $N_c = \text{const}$  and  $q = \text{const}$ , the parameters  $R_c$  and  $D_c$  can depend on the conformation of the substituting side fragments  $\Phi$ . The transitions **9b(1, 2)  $\rightarrow$  9b(3, 4)**, **9c(1, 2)  $\rightarrow$  9c(1/3, 2/3, 1/4, 2/4)**, **10b(1/5, 2/6)  $\rightarrow$  10b(1/8, 2/7)**, and **10c(1/5, 2/6)  $\rightarrow$  10c(1/8, 2/7)** are accompanied by an increase in the parameter  $R_c$  and a decrease in the quantity  $D_c$ . On the other hand, the transitions **9b(3, 4)  $\rightarrow$  9b(1/3, 2/3, 1/4, 2/4)** and **10b(1/8, 2/7)  $\rightarrow$  10b(3/6, 4/5)** result in an increase in the parameter  $D_c$  for the former transitions and in a decrease in this parameter for the latter transitions at the same values of  $R_c$ . In these cases, when the parameter  $R_c$  varies insignificantly, the quantity  $D_c$  is predominantly determined by the density of infill of the core area with atoms of the substituting fragments  $\Phi$ .

The correlation between the parameters  $\rho_c$  and  $D_c$  in expression (3) for all the studied compounds and their conformers is illustrated in Fig. 5. Without regard for the molecules  $NPh$  ( $N = 2, 4, 6$ ), the dependence shown in Fig. 5 can be approximated by the relationship

$$\rho_c = b - fD_c \quad (4)$$

with parameters  $b = 3.186$  and  $f = 1.378$  and a correlation coefficient of 0.985. At  $D_c = 1$ , the density  $\rho_c =$

1.808 exceeds  $\rho_c = 1$  for a linear chain of spheres and reflects the specific features of the chemical structure of the cores in lathlike mesogenic molecules of types **1** and **7** with planar bridging fragments and (or) phenyl rings, which are responsible for the increase in the parameter  $\rho_c$ . At  $D_c = 2$ , the atomic packing density in the cores of the model molecules under consideration  $\rho_c = 0.430$  is half as high as the density  $\rho_c = \pi/(12)^{1/2} \approx 0.907$  for a close hexagonal packing of spheres in the plane at  $R \gg r$  [2]. For molecules  $NPh$  ( $N = 2, 4, 6$ ), the dependence shown in Fig. 5 can be approximated by relationship (4) with parameters  $b = 3.349$  and  $f = 1.657$  and a correlation coefficient of 0.999. According to this dependence, the density  $\rho_c(D_c = 1) = 1.692$  appears to be close to that for the other compounds.

#### 4. DIMENSION OF MOLECULES IN THE REGION OF SIDE CHAINS

It can be seen from Figs. 4 and 6 that, for all the studied compounds and their conformers, the dependence of  $\log N(R)$  on  $\log R$  in the range  $R > R_c$  exhibits an almost linear behavior and, to a first approximation, can be represented in the form

$$\log N(R) = a_{ch} + D_{ch} \log R \quad (5)$$

with constant parameters  $a_{ch}$  and  $D_{ch}$ . The effective mass dimensions  $D_{ch}$  of molecules in the chain region were obtained by averaging over the length of the chain containing 16 atoms (Table 2). As can be seen from Table 2, the dimensions  $D_{ch} < 1$  and  $D_{ch} > 1$  are observed for different compounds.

At  $R_c = \text{const}$ , an increase in the parameter  $N_c$  and the number  $q$  of chains per molecule in the series of compounds **1–2–3–4** leads to a monotonic increase in the dimension  $D_{ch} < 1$ . A similar increase in the parameter  $D_{ch}$  is observed with an increase in the number of chains from two (four) to six upon transition **7**  $\rightarrow$  **8** (**5**  $\rightarrow$  **6**). Therefore, owing to the denser infill of the spherical layer between the spheres of radii  $R_c$  and  $R$  with chains due to an increase in their number, the dimension  $D_{ch}$  tends to 1.

For molecules  $nNPh$ , an increase in the parameters  $N$ ,  $N_c$ , and  $R_c$  results in a monotonic decrease in the dimension  $D_{ch} < 1$ . A similar regularity is observed upon transitions **6**  $\rightarrow$  **4** (**5**  $\rightarrow$  **3**) and **9b**(1, 2)  $\rightarrow$  **9c**(1, 2). Upon transitions **9b**(1/3, 2/3)  $\rightarrow$  **9c**(1/3, 2/3), **9b**(1/4, 2/4)  $\rightarrow$  **9c**(1/4, 2/4), and **10b**(3/6, 4/5)  $\rightarrow$  **10c**(3/6, 4/5), the inequality  $D_{ch} > 1$  is reversed. This indicates that the dimension  $D_{ch}$  depends strongly on the parameters  $N_c$  and  $R_c$ . For effective dimensions  $D_{ch} < 1$  ( $D_{ch} > 1$ ), the derivative  $D(R)$  [relationship (1)] increases (decreases) insignificantly with an increase in  $R$  and tends to unity.

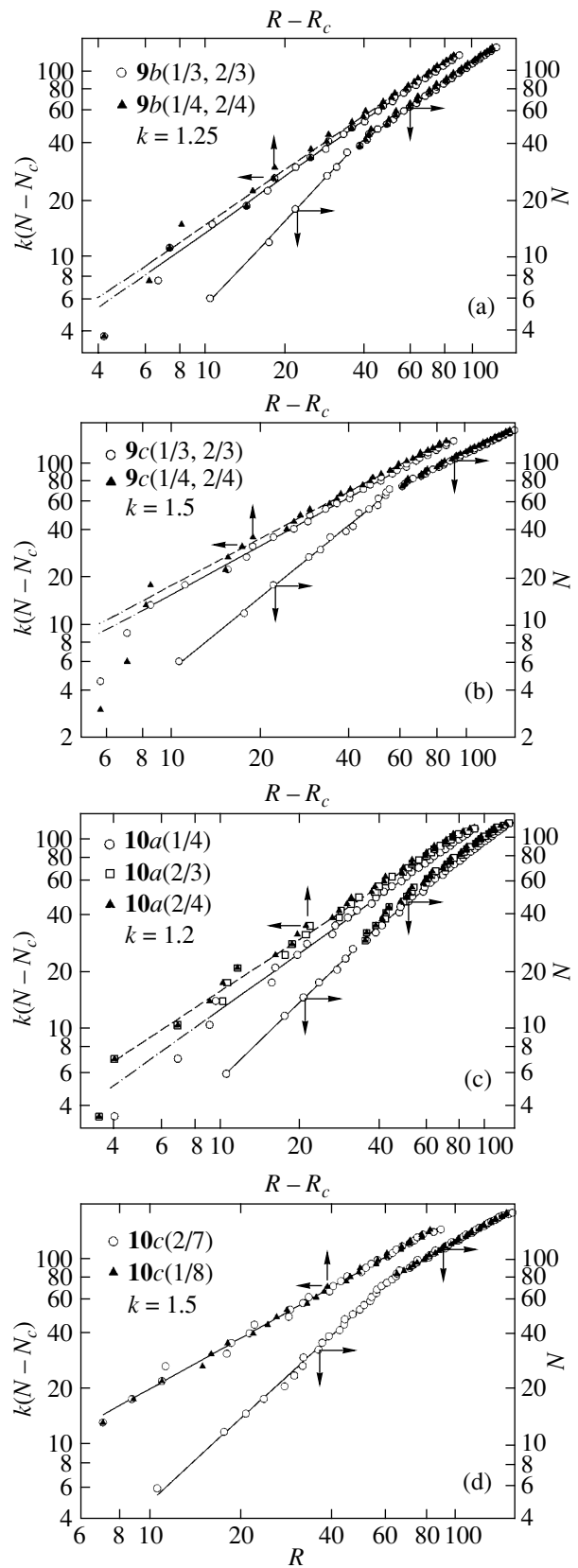


**Fig. 6.** Dependences of the parameters  $N(R)$  and  $k(N - N_c)$  on  $(R - R_c)$  for the studied compounds.

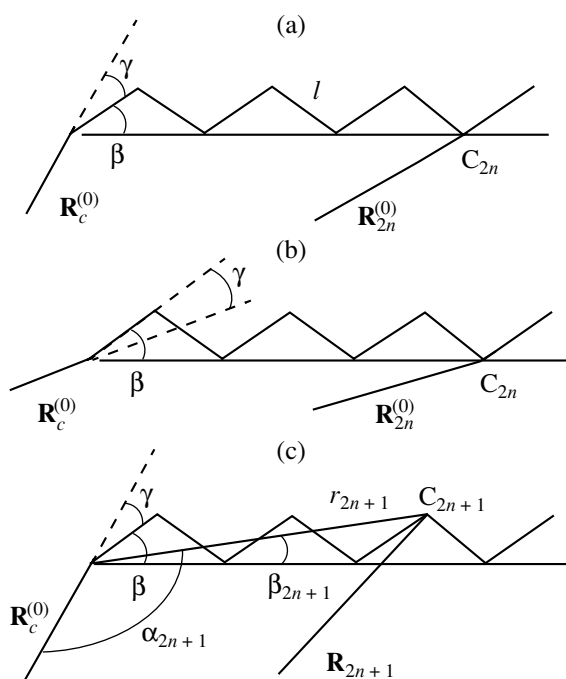


Fig. 7. Relative positions of the vectors  $\mathbf{R}_c^{(0)}$  and  $\mathbf{R}_p^{(0)}$  and the carbon backbone of the chain.

In the range  $R > R_c$ , we introduce the derivative

$$b_{ch}(R) = \frac{d \ln [N(R) - N_c]}{d \ln (R - R_c)}. \quad (6)$$

The dependences of  $\log[N(R) - N_c]$  on  $\log(R - R_c)$  for a number of compounds are plotted in Fig. 6. These dependences for the homologs with  $n > 2$  exhibit a nearly linear behavior and are approximated well by the expression

$$\log [N(R) - N_c] = C_{ch} + b_{ch} \log (R - R_c) \quad (7)$$

with constant parameters  $C_{ch}$  and  $b_{ch}$ . The effective values of  $b_{ch}$  are presented in Table 2. For the majority of compounds, the inequality  $b_{ch} \leq 1$  is satisfied and the differences between the values of  $b_{ch} > 1$  and unity are within the error in determining  $b_{ch}$ . It is seen that the studied compounds satisfy both inequalities  $D_{ch} < b_{ch}$  and  $D_{ch} > b_{ch}$  and the equality  $D_{ch} = b_{ch}$  [for molecules **9b(1)**, **9b(2)**]. Using compounds  $n2Ph-n4Ph$  as an example, it can be shown that the sensitivity of the quantity  $b_{ch}$  to variations in the parameters  $N_c$  and  $R_c$  is less than the sensitivity of the quantity  $D_{ch}$ . At  $R_c = \text{const}$ , an increase in the parameter  $N_c$  and in the number  $q$  of chains per molecule in the series of compounds **1-2-3-4** has no effect on the quantity  $b_{ch}$ , as is the case with the transition **7**  $\rightarrow$  **8** (**5**  $\rightarrow$  **6**). For all the compounds and their conformers, the dependence of the quantity  $b_{ch}$  on the conformation of the side core frag-

ments and chains is substantially more pronounced than the corresponding dependence of the quantity  $D_{ch}$ .

Now, we turn to the explanation of the features revealed in the dependences of  $D(R)$ ,  $D_{ch}$ ,  $b_{ch}(R)$ , and  $b_{ch}$ . Let us consider a lacunar (lathlike) molecule with a statistical symmetry axis  $C_k$  ( $k \geq 2$ ) that passes through the center of the molecular core perpendicularly to the core plane (i.e., normally to the longitudinal axis of the core). We assume that each of  $q$  core fragments related by the symmetry axis  $C_k$  has  $m$  side chains and each chain adopts a specific conformation. Then, within the cluster model for the molecule whose chains are located in the region  $R > R_c$ , we can write the relationship

$$N(R) = N_c + \frac{q}{2r} (R - R_c) \sigma(R). \quad (8)$$

The function  $\sigma(r)$  is defined by the expression

$$\sigma(R) = \sum_{i=1}^m \kappa_p^{(i)}(R), \quad (9)$$

where the index  $i$  numbers the chains in a particular core fragment and  $p$  is the parity index of the C atoms in the chain. The function  $\kappa_p^{(i)}(R)$ , whose properties will be considered below, depends on the chain conformation and the angle between the axis of the chain in a *trans* conformation and the radius vector  $\mathbf{R}_c^{(0)}$  that connects the center of the core to the center of the  $C_0$  atom to which the chain is bonded. From expression (8), we obtain the relationship

$$\sigma(R) = \frac{2r [N(R) - N_c]}{q(R - R_c)}, \quad (10)$$

which can be conveniently used for determining the function  $\sigma(R)$  from the results of the computer simulation.

From formula (6) with due regard for expression (8), we find

$$b_{ch}(R) = 1 + (R - R_c) \frac{d \ln \sigma(R)}{dR}. \quad (11)$$

As will be shown below, for chains that adopt a *trans* conformation and do not make very large angles with the radius vector  $\mathbf{R}_c^{(0)}$ , the decreasing function  $\sigma(R)$  is weakly pronounced and tends to a limiting value with an increase in the parameter  $R$ . Therefore, we have the inequality  $b_{ch}(R) \leq 1$  and find that the quantity  $b_{ch}(R)$  tends to unity with an increase in  $R$ . For the homologs with  $n$  in the range  $2 \leq n \leq 16$ , the increase in the difference  $(R - R_c)$  with an increase in  $n$  in formula (11) compensates for the decrease in the quantity  $\sigma(R)$ . This explains the approximate equality  $b_{ch}(R) \approx b_{ch}$  and the observed dependence described by relationship (7).

**Table 2.** Parameters  $N_c$ ,  $R_c$ ,  $\rho_c$ ,  $D_c$ ,  $D_{ch}$ , and  $b_{ch}$  determined from computer simulation of molecules of the compounds under consideration for different conformations of side fragments

Compound	<i>n2Ph</i>	<i>n3Ph</i>	<i>n4Ph</i>	<b>1(1)</b>	<b>1(2)</b>	<b>2(1)</b>	<b>2(2)</b>	<b>3(1)</b>
$N_c(R_c)$	12(21)	18(31.5)	24(42)	24(42.8)		33(42.8)		42(42.8)
$\rho_c$	0.679	1.793	1.463	1.833		1.452		1.233
$D_c$	1.612	1.025	1.128	0.998		1.224		1.391
$D_{ch}$	0.814	0.786	0.769	0.770	0.780	0.813	0.821	0.837
$b_{ch}$	0.973	0.973	0.977	0.993	0.959	0.993	0.959	0.993
Compound	<b>3(2)</b>	<b>4(1)</b>	<b>4(2)</b>	<b>5(1)</b>	<b>5(2)</b>	<b>6(1)</b>	<b>6(2)</b>	8
$N_c(R_c)$	42(42.8)	60(42.8)		20(22)		24(22)		54(45.5)
$\rho_c$	1.233	0.989		1.026		0.799		1.090
$D_c$	1.391	1.634		1.582		1.788		1.489
$D_{ch}$	0.844	0.862	0.868	0.904	0.879	0.995	0.959	0.933
$b_{ch}$	0.959	0.993	0.959	1.011	0.923	1.011	0.923	0.967
Compound	<b>9a</b>	<b>9b(1)</b> <b>9b(2)</b>	<b>9b(3)</b>	<b>9b(4)</b>	<b>9b(1/3)</b> <b>9b(2/3)</b>	<b>9b(1/4)</b> <b>9b(2/4)</b>	<b>9c(1)</b> <b>9c(2)</b>	<b>9c(1/3)</b> <b>9c(2/3)</b>
$N_c(R_c)$	18(22)	36(31.5)	36(34.3)		36(34.3)		72(53.2)	72(54.5)
$\rho_c$	1.186	0.944	1.166		1.122		1.050	1.116
$D_c$	1.464	1.630	1.472		1.503		1.561	1.503
$D_{ch}$	1.109	0.973	1.005	1.018	1.009	1.017	0.890	0.899
$b_{ch}$	1.011	0.973	0.983	0.914	0.999	0.971	0.970	1.010
Compound	<b>9c(1/4)</b> <b>9c(2/4)</b>	<b>9d(1)</b>	<b>9d(2)</b>	<b>10a(1/4, 2/3, 2/4)</b>	<b>10b(1/5)</b>	<b>10b(2/6)</b>	<b>10b(2/7)</b>	<b>10b(1/8)</b>
$N_c(R_c)$	72(54.5)	66(56.7)		27(31.5)	45(41.6)		45(43.1)	
$\rho_c$	1.116	1.334		1.389	1.133		1.188	
$D_c$	1.503	1.367		1.339	1.466		1.438	
$D_{ch}$	0.922	0.966	0.984	$1 < D_{ch} \leq D_c$	0.988	0.984	0.973	1.009
$b_{ch}$	0.975	0.983	0.949	0.993*	0.930	0.874	0.892	0.931
Compound	<b>10b(3/6)</b>	<b>10b(4/5)</b>	<b>10c(1/5)</b>	<b>10c(2/6)</b>	<b>10c(2/7)</b>	<b>10c(1/8)</b>	<b>10c(3/6)</b>	<b>10c(4/5)</b>
$N_c(R_c)$	45(43.1)		81(62.8)		81(63.7)		81(62.8)	
$\rho_c$	1.299		1.052		1.077		1.098	
$D_c$	1.377		1.506		1.491		1.466	
$D_{ch}$	1.016	$1 < D_{ch} \leq D_c$	0.891	0.895	0.881	0.906	0.901	0.931
$b_{ch}$	0.995	0.913	0.955	0.853	0.908	0.932	1.011	0.956

\* For molecules **10a(2/3)** and **10a(2/4)**,  $b_{ch} = 0.914$ .

Substituting expression (8) into formula (1) gives the relationship

$$D(R) = \frac{R[N(R) - N_c]}{N(R)(R - R_c)} b_{ch}(R) \equiv D_0(R) b_{ch}(R). \quad (12)$$

At  $R \gg R_c$  and  $N(R) \gg N_c$ , we have  $D_0(R) \approx 1$  and  $D(R) \approx b_{ch}(R)$ . By disregarding the dependence  $\sigma(R)$ , from formula (10), we obtain the relationship  $[N(R) - N_c] \sim (R - R_c)$  and the equality  $D(R) = D_0(R)$ . Setting

$[N(R) - N_c]/(R - R_c) \equiv \tan \alpha$  and  $N(R)/R \equiv \tan \theta(R)$ , we can write the expression for  $D_0(R)$  in the form

$$D_0(R) = \tan \alpha / \tan \theta(R). \quad (13)$$

At  $\alpha < \theta(R)$ , the inequality  $D_0(R) < 1$  is satisfied for the majority of the studied compounds. At  $\alpha > \theta(R)$ , we have the inequality  $D_0(R) > 1$  for molecules **9a**, **9b(3, 4, 1/3, 2/4)**, **10a(1/4, 2/3, 2/4)**, and **10b(1/8, 3/6, 4/5)**. At  $\alpha < \theta(R)$  [ $\alpha > \theta(R)$ ], an increase in  $R$  leads to a slow decrease (increase) in the angle  $\theta(R)$  tending to the

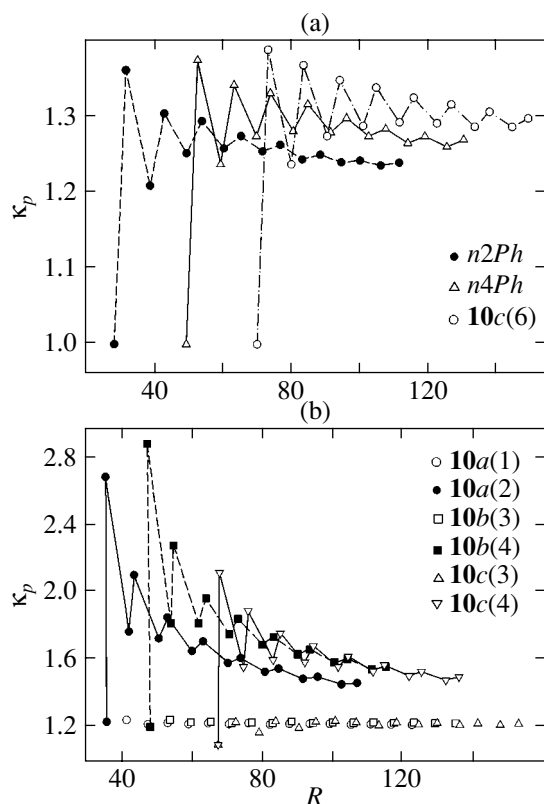


**Fig. 8.** Dependences  $\kappa_p(R)$  for the studied compounds with (a)  $\gamma = 0$  and (b) different values of  $\beta - \gamma$ . For explanation, see the text.

angle  $\alpha$  and an increase (decrease) in the quantity  $D_0(R)$  tending to unity. The dependence  $D_0(R)$  can be well pronounced for molecules with small values of  $N_c$  and  $R_c$ . This is actually observed for compounds *n2Ph*, **5**(1, 2), **9a**, and **10a**(1/4, 2/3, 2/4).

At  $D_0(R) < 1$ , the insignificant decrease in the function  $\ln\sigma(R)$  with an increase in  $R$  in relationships (11) and (12) partially compensates for the increase in  $D_0(R)$  with an increase in the chain length and is responsible for the observed approximate equality  $D(R) \approx D_{ch} < 1$ . By contrast, at  $D_0(R) > 1$ , the decrease in the function  $\ln\sigma(R)$  with an increase in  $R$  in relationships (11) and (12) enhances the decrease in  $D(R)$  with an increase in the chain length. This is characteristic of molecules **9a** and **10b**(4/5) and can be seen in Fig. 6c for molecules **10a**(1/4, 2/3, 2/4).

The same limiting value  $D_{ch}(n \rightarrow \infty) = 1$  obtained for lathlike and lacunar nematic molecules with long side chains suggests that, in the limit, these molecules are isomorphic with respect to the quantity  $D_{ch}$ . This explains the close limiting temperatures  $T_l = T_c(n \rightarrow \infty)$  of the  $N_D$ -I phase transition with an increase in the length of only one chain in molecule **8** or all chains in molecule **9c** [17].

Let us analyze the basic properties of the function  $\kappa_p^{(i)}(R)$  for even and odd homologs with the chains in the *trans* conformation. For simplicity, we assume that the carbon backbone of the chain, the vector  $\mathbf{R}_c^{(0)}$ , and the vector  $\mathbf{R}_{2n}^{(0)}$  ( $\mathbf{R}_{2n+1}^{(0)}$ ) connecting the core center to the center of the even (odd) atom in the chain lie in the same plane. The arrangement of these vectors is schematically depicted in Fig. 7. For the even atoms in the chain, we have the exact expression

$$R_{2n}^{(0)} = [\mathbf{R}_c^{(0)} + r_{2n}] \left\{ 1 - \frac{2r_{2n}R_c^{(0)}[1 - \cos(\beta \pm \gamma)]}{[\mathbf{R}_c^{(0)} + r_{2n}]^2} \right\}^{1/2}, \quad (14)$$

where  $r_{2n} = 2nl\cos\beta$  is the distance between the centers of the  $C_0$  and  $C_{2n}$  atoms. The signs “+” and “-” ahead of  $\gamma$  corresponds to the schemes shown in Figs. 7a and 7b, which differ from each other by the rotation of the chain around the  $C_0$ - $C_1$  bond through an angle of  $180^\circ$ .

With due regard for the inequality  $2r_{2n}R_c^{(0)}/[\mathbf{R}_c^{(0)} + r_{2n}]^2 \leq 1/2$  at  $\gamma = 0$ , we have  $\cos\beta = (2/3)^{1/2}$  and  $(1 - \cos\beta) \approx 0.184$ . Then, expression (14) can be reduced to the approximate relationship

$$R_{2n}^{(0)} = R_c^{(0)} + r_{2n} \frac{2nl\cos\beta + R_c^{(0)}\cos(\beta \pm \gamma)}{2nl\cos\beta + R_c^{(0)}}, \quad (15)$$

which is better satisfied at large differences between  $r_{2n}$  and  $R_c^{(0)}$  and also at  $[1 - \cos(\beta - \gamma)] \ll 1$ . Making allowance for the expressions  $R_{2n} = r + R_{2n}^{(0)}$ ,  $R_c = r + R_c^{(0)}$ , and  $2r = l$  and formula (15), from the relationship

$$2n = \kappa_{2n}(R_{2n} - R_c)/l \quad (16)$$

we obtain

$$\kappa_{2n} = \frac{2nl\cos\beta + R_c^{(0)}}{\cos\beta[2nl\cos\beta + R_c^{(0)}\cos(\beta \pm \gamma)]} \quad (17)$$

$(n \geq 1).$

From relationship (17) for  $\cos\beta = (2/3)^{1/2}$ , we find that the inequalities  $\kappa_{2n} \geq (3/2)^{1/2} \approx 1.225$  and  $\kappa_{2n} < 3/2$  at  $\gamma = 0$  are satisfied,  $\kappa_{2n}$  monotonically decreases and tends to  $(3/2)^{1/2}$  with an increase in  $n$  or a decrease in the difference  $(\beta - \gamma)$  at fixed  $n$ , and  $\kappa_{2n}$  increases with an increase in the sum  $(\beta + \gamma)$  or the ratio  $R_c^{(0)}/l$ . At  $\beta - \gamma = 0$ , all the even atoms in the chain lie in the extension of the vector  $\mathbf{R}_c^{(0)}$  and  $\kappa_{2n} = (3/2)^{1/2}$ . Therefore, at  $0 \leq (\beta - \gamma) \leq \beta$ , the function  $\kappa_{2n}(R)$  is a decreasing function and the values of  $\kappa_{2n}(R)$  fall in a narrow

range; hence, the dependence  $\kappa_{2n}(R)$  in expression (9) can be ignored.

For odd atoms in the chain, we first consider the case where  $\gamma = 0$ . In the same approximation as for formula (15), we can write the relationship

$$R_{2n+1}^{(0)} = R_c^{(0)} + l + r_{2n} \cos \beta \frac{(2n+1)l + R_c^{(0)}}{2nl \cos \beta + R_c^{(0)} + l}, \quad (18)$$

which differs from formula (15) at  $\gamma = 0$  in the substitution of  $R_c^{(0)} + l = R_1^{(0)}$  for  $R_c^{(0)}$ . With allowance made for the equality  $R_{2n+1} = r + R_{2n+1}^{(0)}$  and expression (18), from relationship

$$\begin{aligned} 2n+1 &= \kappa_{2n+1}(R_{2n+1} - R_c)/l \\ &= \kappa_{2n+1}[(R_{2n+1} - R_1)/l + 1] \end{aligned} \quad (19)$$

we obtain

$$\kappa_{2n+1} = (2n+1) \left[ 1 + (2n \cos^2 \beta) \frac{(2n+1)l + R_c^{(0)}}{2nl \cos \beta + l + R_c^{(0)}} \right]^{-1} \quad (20)$$

For  $n = 0$ , we have  $\kappa_1 = 1$ . This explains the deviation of  $\log[N(R) - N_c]$  from the linear dependence [described by formula (7)] in Figs. 6a–6c for the first homologs of compounds having conformers with  $\gamma = 0$ . In relationship (20), the fractional expression in brackets varies in the range from 1 to  $(3/2)^{1/2}$  and, at  $n \gg 1$ , relationship (20) is reduced to the following formula:

$$\kappa_{2n+1} = (3/2) \frac{[2n(2/3)^{1/2} + 1]l + R_c^{(0)}}{(2n+1)l + R_c^{(0)}}. \quad (21)$$

For  $2n(2/3)^{1/2} \gg [1 + R_c^{(0)}/l]$ , the function  $\kappa_{2n+1}$  tends to  $(3/2)^{1/2}$ . In the case of the reverse inequality  $[1 + R_c^{(0)}/l] \gg 2n$ , according to relationship (20), the function  $\kappa_{2n+1} = 3(2n+1)/(4n+3)$  monotonically increases

with an increase in  $n$ . In particular, we have  $\kappa_3 = 9/7 \approx 1.286 > (3/2)^{1/2}$ . This indicates that the function  $\kappa_{2n+1}$  [relationship (20)] varies nonmonotonically with an increase in  $n$  (i.e., it has a maximum).

For  $\gamma \neq 0$ , it can be seen from the scheme shown in Fig. 7c that  $\alpha_{2n+1} = \pi - (\beta \pm \gamma) + \beta_{2n+1}$ . As a result, at  $[1 - \cos(\beta \pm \gamma - \beta_{2n+1})] \ll 1$ , we obtain

$$\begin{aligned} &R_{2n+1}^{(0)} \\ &= R_c^{(0)} + r_{2n+1} \frac{r_{2n+1} + R_c^{(0)} \cos(\beta \pm \gamma - \beta_{2n+1})}{r_{2n+1} + R_c^{(0)}}. \end{aligned} \quad (22)$$

Substituting this expression into formula (19) gives the relationship

$$\kappa_{2n+1} = \frac{l(2n+1)}{r_{2n+1}} \left[ \frac{r_{2n+1} + R_c^{(0)}}{r_{2n+1} + R_c^{(0)} \cos(\beta \pm \gamma - \beta_{2n+1})} \right]. \quad (23)$$

For  $n = \gamma = 0$ , we have  $r_1 = l$ ,  $\beta_1 = \beta$ , and  $\kappa_1 = 1$ . At  $n = \beta - \gamma = 0$  and  $R_c^{(0)} \gg l$ , we obtain  $\kappa_1 = (3/2)^{1/2}$ . In the case of  $n > 1$ , the following relationships are satisfied to a high accuracy:

$$\begin{aligned} r_{2n+1} &= l(2n+1) \cos \beta [1 + \tan^2 \beta / (2n+1)^2]^{1/2} \\ &\approx l(2n+1)(2/3)^{1/2} [1 + (1/4)/(2n+1)^2], \\ \cos(\beta \pm \gamma - \beta_{2n+1}) &= \frac{l(2n+1) \cos \beta}{r_{2n+1}} [\cos(\beta \pm \gamma) \\ &+ \frac{\tan \beta}{(2n+1)} \sin(\beta \pm \gamma)] \approx [1 + (1/4)/(2n+1)^2]^{-1} \\ &\times \left[ \cos(\beta \pm \gamma) + \frac{1}{(2n+1)\sqrt{2}} \sin(\beta \pm \gamma) \right]. \end{aligned} \quad (24)$$

With allowance made for relationships (24) at  $4(2n+1)^2 \gg 1$  (this inequality is valid even at  $n = 1$ ), formula (23) takes the form

$$\kappa_{2n+1} = \frac{(2n+1)l \cos \beta + R_c^{(0)}}{\cos \beta \{ (2n+1)l \cos \beta + R_c^{(0)} [\cos(\beta \pm \gamma) + \sin(\beta \pm \gamma)/\sqrt{2}(2n+1)] \}}. \quad (25)$$

For larger values of  $n$  satisfying the inequality  $(2n+1) \gg 1$ , formula (25) differs from formula (17) in the substitution of  $(2n+1)$  for  $2n$  and all the results obtained for formula (17) are valid for formula (25). In particular, for these values of  $n$  and  $\cos \beta = (2/3)^{1/2}$ , the inequality  $\kappa_{2n+1} \geq (3/2)^{1/2}$  is satisfied, while at  $(\beta - \gamma) = 0$ , we have  $\kappa_{2n+1} = (3/2)^{1/2}$ . By ignoring the term  $\sim \sin(\beta \pm \gamma)$  in the denominator of formula (25), i.e., by using the overestimated value of  $\kappa_{2n+1}$  and comparing

it with formula (17), it can be shown that  $\kappa_{2n+1} < \kappa_{2n}$ . The branch of the  $\kappa_{2n+1}$  values lies below the branch of the  $\kappa_{2n}$  values at all  $n$ . Therefore, at  $n \geq 1$  and  $0 \leq (\beta - \gamma) \leq \beta$ , the nonmonotonic function  $\kappa_{2n+1}(R)$  varies in a narrow range and the dependence  $\kappa_{2n+1}(R)$  in expression (9) can be ignored with a high accuracy.

Figure 8 depicts the exact dependences  $\kappa_p(R)$  calculated from relationships (16) and (19) for a number of molecules and their conformers at different values of

( $\beta \pm \gamma$ ). It can be seen from Fig. 8 that all the aforementioned qualitative and quantitative results obtained from expressions (17), (20), (21), (23), and (25) are valid for molecules  $n2Ph$ ,  $n4Ph$ , and **10c(6)** with  $\gamma = 0$  and the parameters  $\lambda = R_c^{(0)}/l = 2.5, 5.5, \text{ and } 8.5$ , respectively; conformers **10a(1)** and **10b(3)** with  $\beta - \gamma \approx 0$  and  $\lambda = 3.7$  and  $5.5$ , respectively; and conformer **10c(3)** with  $\beta - \gamma > 0$  and  $\lambda = 8.2$ . Note that we have  $i = 1$  and  $\kappa_p(R) = \sigma(R)$  in formula (9) for molecules  $nNPh$ .

In the above case where  $0 \leq (\beta - \gamma) \leq \beta$ , the dependence  $\sigma(R)$  described by relationship (9) is also weak and can be disregarded. This explains the good agreement between the effective parameters  $D_{ch}$  obtained from relationship (5) and the values of  $\langle D_0(R) \rangle$  calculated from expression (12) and averaged over all homologs of the studied molecules and conformers satisfying the condition  $0 \leq (\beta - \gamma) \leq \beta$ .

The quantitative results of the analytical treatment performed are not applicable to conformers **10a(2)** and **10b(4)** with  $\beta + \gamma \approx 2\beta$ . It can be seen from Fig. 8b that, for these conformers, the values of  $\kappa_p(R)$  considerably increase for the first homologs and the values of  $\kappa_{2n}(R)$  [ $\kappa_{2n+1}(R)$ ] decrease monotonically [nonmonotonically, with passing through a maximum] more rapidly than those in Fig. 8a with an increase in  $n$  and  $R$ . The presence of such conformers in molecules favors a leading increase in the values of  $N(R)$  represented by expression (8) for the first homologs and results in an increase in the parameters  $D_0(R)$  and  $D(R)$  described by formula (12). This explains the results of the numerical experiment for molecules **10a(2/3, 2/4)** (Fig. 6c) and **10b(4/5)** involving these conformers, for which the dependence of  $\log N(R)$  on  $\log R$  is hump-shaped with  $D(R) \approx D_c$  for the first chain homologs and exhibits a rapid decrease in the parameters  $D(R)$  with an increase in the chain length. For molecule **10c(4/5)** including conformer **10c(4)** with smaller values of  $\gamma$  and  $(\beta + \gamma) < 2\beta$ , the dependence of  $\log N(R)$  on  $\log R$  is also hump-shaped, but it is less pronounced.

The ignored thermal conformational mobility of chains should lead to an increase in the values of  $\sigma(R)$ ,  $b_{ch}(R)$ , and  $D(R)$  due to the smearing of the region of location of chain atoms in the directions perpendicular to the vectors  $\mathbf{R}_p^{(0)}$  and the leading increase in  $N(R)$  as compared to  $R$  in formula (10). This situation is qualitatively similar to the above situation associated with the increase in the sum  $(\beta + \gamma)$  for the chain in the *trans* conformation. For molecules of type **1** and **7**, the presence of the chains in the *ortho* positions of the terminal phenyl rings [with respect to the  $-\text{C}(\text{O})\text{O}-$  and  $-\text{C}\equiv\text{C}-$  bridging fragments] should assist the filing of lacunas of the core and the increase in the dimension  $D_c$ . This is important from the standpoint of the design of biaxial molecules capable of forming a biaxial thermotropic nematic phase  $N_b$ .

Now, we consider the mean density of atoms  $\bar{\rho}(R) = N(R)/V(R)$  in the volume of a sphere  $V(R) = 4\pi R^3/3$  and the differential (local) density of atoms  $\rho(R) = dN(R)/dV(R)$  in the volume of a spherical layer  $dV(R) = 4\pi R^2 dR$ . These densities are related by the expression

$$\rho(R) = D(R)\bar{\rho}(R)/3 \quad (26)$$

and coincide with each other at  $D(R) = \text{const} = 3$ . In the region of molecular cores, when relationship (3) is satisfied and at  $1 < D_c < 2$ , the densities  $\rho(R) \sim \bar{\rho}(R) \sim R^{D_c-3}$  decrease with an increase in  $R$  ( $R \leq R_c$ ). In the region of side chains, with due regard for formula (8), we have

$$\bar{\rho}(R) = \frac{3}{4\pi} \left\{ \frac{q\sigma(R)}{2rR^2} + \frac{1}{R^3} [N_c - qR_c\sigma(R)/2r] \right\}. \quad (27)$$

According to expression (27), the densities  $\bar{\rho}(R)$  and  $\rho(R)$  decrease even more rapidly with an increase in  $R$  due to the weak dependence  $\sigma(R)$ . Therefore, the mass density of an isolated lacunar molecule  $\rho_M \sim M(R_M)/V(R_M) \sim \bar{\rho}(R_M)$  rapidly decreases with an increase in the radius  $R_M$  of the sphere containing the molecule. However, the density  $\rho = m/v$  ( $m$  is the molecular weight,  $v$  is the molar volume) of discotic nematic phases  $N_D$  is identical to the density of calamitic nematic liquid crystals with a relatively close packing of lathlike molecules. This implies that, in the  $N_D$  phase, molecules should mutually penetrate into each other and lacunas of a particular molecule should be filled with side chains of neighboring molecules (similar to engaged gears). As a consequence, discotic nematic liquid crystals should possess a high viscosity which is actually one or two orders of magnitude higher than the viscosity of calamitic nematic liquid crystals [18, 19].

## 5. CONCLUSIONS

Thus, the results obtained in this work have demonstrated that, for a large number of lathlike and lacunar mesogenic molecules (and their conformers) with different chemical structures, the dependence of  $\log N(R)$  on  $\log R$  exhibits two linear portions that correspond to the core region ( $R \leq R_c$ ) and the region of side chains ( $R_c < R \leq R_M$ ). Moreover, these portions correspond to the mass dimensions  $1 < D_c < 2$  and  $D_{ch} \leq 1$  or  $D_{ch} \geq 1$ , depending on the chain conformation. The difference between the dimensions  $D_c$  and  $D_{ch}$  accounts for the fact that, at  $R \leq R_M$ , the molecules under consideration are not self-similar objects and the topological dimension  $D_T = 3$  for these molecules as physical bodies (rather than molecular graphs, i.e., systems of valence bonds connecting the points of atomic positions) is larger than the dimensions  $D_c$  and  $D_{ch}$ . Therefore, the molecules studied are not fractals for which  $D > D_T$  by

definition [1] but belong to a particular class of lacunar objects with a nonuniform (on their size scale) fractional mass dimension  $D < D_T$ . On the other hand, it can be expected that mesogenic molecules of the monodendron and dendrimer types [6, 7] (not discussed in this work), as well as amphiphilic starlike and dendritic molecules [8, 9] with a branching structure of side fragments, which are characterized by a rather close packing in the three-dimensional space, should have by dimensions  $D \leq 3$ .

It was established how the main molecular characteristics (molecular symmetry, the number and size of core fragments, their structural–chemical features and conformation, the length and conformation of side chains) affect the values of  $D_c$  and  $\rho_c$  and the dependence  $b_{ch}(R)$ . The proposed analytical approach to the analysis of the dependences  $D(R)$  and  $b_{ch}(R)$  made it possible to explain all the main results of the numerical simulation of the compounds under investigation. The high sensitivity of the parameters  $D_c$  and  $\rho_c$  to variations in the fine features of the molecular structure indicates that the use of these parameters as descriptors for identifying and predicting the mesogenic properties of molecules in addition to the descriptors already serving for these purposes [16] holds considerable promise.

#### REFERENCES

1. B. B. Mandelbrot, *The Fractal Geometry of Nature* (Freeman, New York, 1983; Inst. Komp. Issled., Moscow, 2002).
2. J. Feder, *Fractals* (Plenum, New York, 1988; Mir, Moscow, 1991).
3. D. Demus, *Liq. Cryst.* **5** (1), 75 (1989).
4. D. Demus, in *Handbook of Liquid Crystals*, Ed. by D. Demus, J. Goodby, H.-W. Spiess, and V. Vill (VCH, London, 1998), Vol. 1, Chap. 6, p. 133.
5. K. Praefcke, *EMIS Datarev. Ser.* **25**, 17 (2000).
6. C. T. Imrie, *EMIS Datarev. Ser.* **25**, 36 (2000).
7. D. Demus, *Mol. Cryst. Liq. Cryst.* **364**, 25 (2001).
8. C. Tschierske, *Annu. Rep. Prog. Chem., Sect. C: Phys. Chem.* **97** (1), 191 (2001).
9. C. Tschierske, *J. Mater. Chem.* **11**, 2647 (2001).
10. C. Destrade, P. Foucher, H. Gasparoux, N. H. Tinh, A. M. Levelut, and I. Malthete, *Mol. Cryst. Liq. Cryst.* **106**, 121 (1984).
11. E. M. Aver'yanov, *Pis'ma Zh. Éksp. Teor. Fiz.* **61** (10), 796 (1995) [*JETP Lett.* **61**, 815 (1995)].
12. E. M. Aver'yanov, *Zh. Éksp. Teor. Fiz.* **110** (5), 1820 (1996) [*JETP* **83**, 1000 (1996)].
13. E. M. Aver'yanov, *Zh. Strukt. Khim.* **38** (1), 89 (1997).
14. E. M. Aver'yanov, *Fiz. Tverd. Tela (St. Petersburg)* **46** (8), 1509 (2004) [*Phys. Solid State* **46**, 1554 (2004)].
15. D. Demus, H. Demus, and H. Zschke, *Flussige Kristalle in Tabellen* (VEB Deutscher Verlag für Grundstoffindustrie, Leipzig, 1974 and 1984), Vols. 1 and 2.
16. O. B. Akopova, O. V. Zemtsova, and N. V. Usol'tseva, *Zhidk. Krist. Ikh Prakt. Ispol.*, No. 1, 25 (2002).
17. E. M. Aver'yanov, *Zhidk. Krist. Ikh Prakt. Ispol.*, No. 1, 25 (2003).
18. T. W. Warmerdam, D. Frenkel, and R. J. J. Zijlstra, *Liq. Cryst.* **3** (8), 1105 (1988).
19. M. Ebert, D. A. Jungbauer, R. Kleppinger, T. H. Wendorff, B. Kohne, and K. Praefcke, *Liq. Cryst.* **4** (1), 53 (1989).

*Translated by O. Borovik-Romanova*